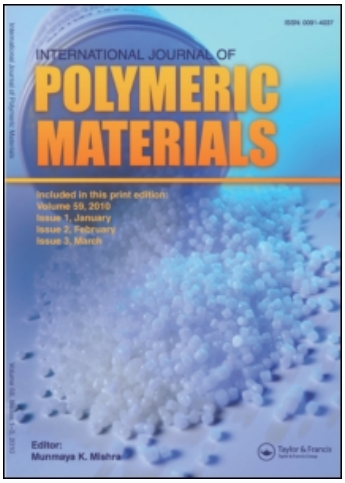

International Journal of Polymeric Materials
Publication details, including instructions for authors and subscription information:
http://www.informaworld.com/smpp/title~content=t713647664

Morphology and finite strain rheologyof NBR/TPU blends

Z. Susteric[a]; I. Dimitrievski[a]
[a] Sava d.d., R & D Institute, Slovenia

Online publication date: 27 October 2010

To cite this Article Susteric, Z. and Dimitrievski, I.(2003) 'Morphology and finite strain rheologyof NBR/TPU blends', International Journal of Polymeric Materials, 52: 6, 527 — 548
To link to this Article: DOI: 10.1080/00914030304908
URL: http://dx.doi.org/10.1080/00914030304908

International Journal of Polymeric Materials, 52: 527–548, 2003

0091-4037/03 $12.00 +.00
DOI: 10.1080/00914030390197789

Taylor & Francis
Taylor & Francis Group

MORPHOLOGY AND FINITE STRAIN RHEOLOGY OF NBR/TPU BLENDS

Z. Susteric
I. Dimitrievski
Sava d.d., R & D Institute, Slovenia

Due to orientational and dispersional interactions between molecules in polar polymer blends, such as NBR/TPU, secondary molecular networks are formed, which, despite their weakness, essentially affect rheological properties of the blends. Being highly susceptible to strain and temperature changes, the secondary networks under such conditions undergo breakdown, causing changes in blends' rheological characteristics. Particularly suitable method for tracking such network breakdown is by measuring the blends' dynamic mechanical functions at different strains and temperatures. For elucidation of these measurements a model is chosen, analysing a secondary network breakdown by statistical mechanics, whose final result is strain, temperature and compositional dependence of the blends' dynamic mechanical functions. Along with the measurements', the chosen model, originally devised to study rheological properties of carbon black filled rubbers, also provides means for quantitative characterization of secondary networks in polar polymeric systems.

Keywords: dynamic mechanical functions, morphology, polar polymer blends, secondary interactions

1. INTRODUCTION

Butadiene-acrylonitrile rubber (NBR) and thermoplastic polyurethane (TPU) are both polar in character and hence, owing to orientational and dispersional interactions [1, 2] in mutual blends, they form associations of NBR-NBR, NBR-TPU and TPU-TPU type. These associations act as multifunctional junctions, or intermolecular linkages in the blends, forming a secondary network that represents their morphological structure when in amorphous state. To the blends'

Received 14 March 2001; in final form 21 March 2001.
Address correspondence to Z. Susteric, Sava d.d., R & D Institute, 4000 Kranj, Slovenia.

morphology also contribute molecular entanglements [3], but as intermolecular linkages these are less expressive in polar systems.

Orientational interactions are of short range and weak in comparison with primary (ionic or covalent) interactions, their energies ranging typically within $5-25\,\mathrm{kJmol}^{-1}$. Nevertheless, rheological properties of polar blends are essentially affected by the multitude of intermolecular linkages produced by orientational interactions, and remarkably, regardless of the blends being uncrosslinked or crosslinked by primary (covalent) linkages.

Weakness of the secondary linkages makes the secondary networks formed in polar blends highly susceptible to strain and temperature changes. This is reflected in strong dependence of the blends' rheological properties on strain and temperature. Already with slight increase in deformation and/or temperature a secondary network undergoes gradual breakdown, but eventually restores and regains its former properties when left at rest. Primary networks, on the other hand, never restore after breakdown, which, however, occurs under much more severe conditions.

Using rather generalized model, previously constructed to explain rheological behaviour of carbon black filled rubbers at low strains [4], the objective of this work is to show relationship between secondary networks in polar NBR/TPU blends and their rheological properties. The model also enables determination of characteristic energies for strain and thermally induced breakdown of the blends' secondary networks, as well as a material constant characteristic of the blends' composition.

2. THEORETICAL

To pursue the foregoing objective, it has proved feasible to study rheological properties of NBR/TPU blends in terms of their morphology by strain, temperature and compositional dependence of the blends' dynamic mechanical functions, *i.e.*, the storage and loss elastic moduli, at a frequency low enough to allow undisturbed changes of molecular conformations in rather broad ranges of strain and temperature. Particularly useful type of deformation for this purpose is oscillating shear strain, since shear moduli are well defined up to rather high strain amplitudes.

Irrespective of deformation type, the storage modulus is by the theory of rubber elasticity proportional to the intermolecular linkage (primary and/or secondary) density and temperature [5]. Taking oscillating shear deformation as an example, Figure 1 schematically demonstrates a typical strain amplitude (γ) dependence of dynamic

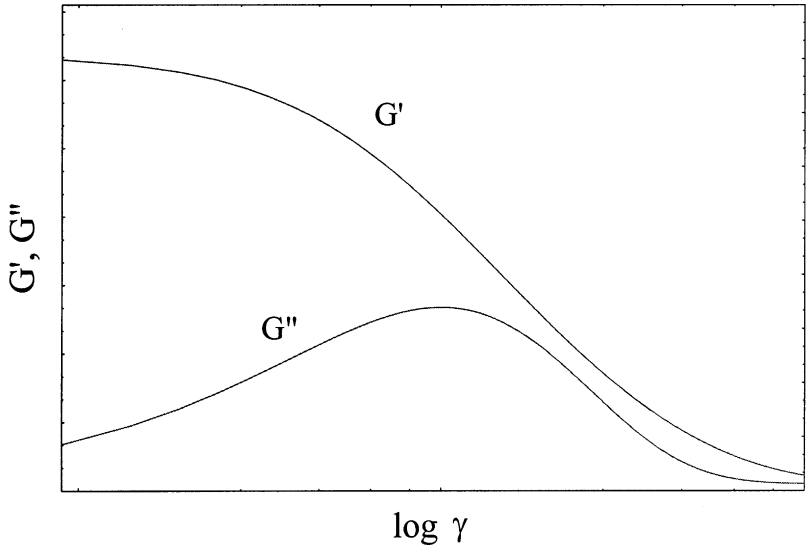

FIGURE 1 Schematically presented dependence of storage and loss shear moduli, G' and G'', on shear strain amplitude.

mechanical functions for materials possessing secondary networks at moderate frequency and temperature.

As the secondary network starts degrading with increasing strain, the secondary linkage density diminishes and the storage shear modulus, G', monotonically decreases from its highest value at zero-strain toward a low but finite terminal value, when the network is completely destroyed.

Since the secondary network breakdown is also an energy dissipation process, the loss shear modulus, G'', being proportional to secondary linkage density change is influenced accordingly. With increasing strain it first increases, reaching its maximum at the strain of the highest secondary network breakdown rate, and then, similarly to the storage modulus, decreases, to attain a low finite value at large strains. It should be mentioned, however, that there is another energy dissipation process, namely the internal friction [6], concurrently occurring in the strained material and affecting its loss modulus. The energy dissipated by this process strongly depends on strain rate.

The effect of temperature on dynamic mechanical functions, on the other hand, is not as straightforward as the one of strain. Although the theory of rubber elasticity, for entropic reasons, predicts G' to be proportional to the temperature, the secondary linkage density decreases with increasing temperature somewhat stronger, making

the net effect a decrease in G'. The same goes for G'', but to its decrease also contributes diminished internal friction. It is important to note that the effect of temperature on G' and G'' gradually decreases with increasing strain and disappears completely at high strains, which is plausible because the secondary network is then thoroughly destroyed.

Such interpretation of dynamic mechanical functions' dependence on strain and temperature seems qualitatively sensible, but in order to quantitatively confirm it, the relevant expressions for G' and G'' should be derived from more primary principles. To achieve this, a model is used, originally devised to describe low strain and temperature dependence of dynamic functions for carbon black filled rubber through quantitative account of the breakdown of black's van der Waals bonded secondary agglomeration network [4]. Generalized for higher strains, the model, based on statistical mechanics of chain molecules and some additional assumptions, has proved to work for polar rubbers, such as NBR and CR (polychloroprene) [7] and seems to perform well for NBR/TPU blends, too.

The adopted assumptions of the model are the following:

(1) Strain induced secondary network breakdown occurs when secondary linkages break and disappear. This happens when linkages are subjected to a certain critical force imposed on them by pendant network chains.
(2) Network chains in a secondary network are of different lengths. The distribution of their *average* chain vectors is assumed to be Gaussian. Hence, upon strain only the chain vectors of chains with a certain length undergo affine transformation, whereas transformation of chain vectors of other chains is nonaffine. Thus for different chains the critical force needed to break a linkage is attained at different strains. Subsequently, at any strain G' is proportional to the density of still existing linkages at that strain, whereas G'' is proportional to the linkage density change at that strain.
(3) The secondary network thermal breakdown is assumed to be a thermally activated process.

2.1. Effect of Strain

From statistical mechanics of chain molecules it is well known that the chain vector distribution in unstrained state, $w_0(\boldsymbol{r})$, is Gaussian, possessing the following form [8]:

$$w_0(\boldsymbol{r}) = (3/2\pi\langle r^2\rangle)^{3/2}\exp(-3r^2/2\langle r^2\rangle), \tag{1}$$

where $r^2 = x^2 + y^2 + z^2$ in Cartesian coordinate system with one end of a network chain in its origin and $\langle r^2\rangle$ is the mean square of the chain vector $\boldsymbol{r}$. For chain vectors transformed affinely in strain, *i.e.*, $\boldsymbol{r} = \{\lambda\}\boldsymbol{r}_0$, where $\{\lambda\}$ is the gradient deformation tensor and $\boldsymbol{r}_0$ the chain vector in unstrained state, the distribution function (1) is transformed accordingly into [8]

$$w(\boldsymbol{r}, \lambda) = (\det\{\lambda\})^{-1} w_0(\{\lambda\}^{-1}\boldsymbol{r}). \tag{2}$$

At low strains, the determinant factor accountable for volume changes can be neglected.

For shear strain, used in this work, the principal values of the tensor $\{\lambda\}$ are $\lambda_1 = \lambda$, $\lambda_2 = 1$ and $\lambda_3 = 1/\lambda$ where λ represents the deformation ratio, *i.e.*, the ratio of specimen's lengths in strained and unstrained state, respectively. Substituting this into Eq. (2) and neglecting the determinant term, distribution of affinely transformed chain vectors turns into

$$w(\boldsymbol{r}, \lambda) = (3/2\pi\langle r^2\rangle_{aff})^{3/2}\exp[-r^2(\lambda^2 + \lambda^{-2} + 1)/2\langle r^2\rangle_{aff})]. \tag{3}$$

Since shear strain is expressible in terms of deformation ratio as $\gamma = \lambda - \lambda^{-1}$ [9], the distribution (3) can be rewritten as a function of γ in the following way:

$$\begin{aligned} w(\boldsymbol{r}, \gamma) &= (3/2\pi\langle r^2\rangle_{aff})^{3/2}\exp[-(3 + \gamma^2)r^2/2\langle r^2\rangle_{aff})] \\ &= w_0(\boldsymbol{r})\exp(-\gamma^2 r^2/2\langle r^2\rangle_{aff}). \end{aligned} \tag{4}$$

As assumed, network linkages break when subjected to a certain critical force. According to statistical mechanics of a single chain, the elastic force deforming the chain is proportional to the corresponding chain vector [5], *i.e.*, $\boldsymbol{f} = 3kT\boldsymbol{r}/\langle r^2\rangle$ where T is the temperature and k the Boltzmann constant. The needed critical force, $\boldsymbol{f}_c$, to break a secondary linkage is then proportional to a certain critical chain vector, $\boldsymbol{r}_c$, and given as

$$\boldsymbol{f}_c = 3kT\boldsymbol{r}_c/\langle r^2\rangle. \tag{5}$$

The fraction of unbroken linkages with pendant network chains of affinely transformed chain vectors at deformation γ, $n_{aff}(\gamma)$, is simply

given by the fraction of chains whose chain vectors do not exceed the critical chain vector $\boldsymbol{r}_c$. Using distribution (4), this fraction is given as

$$n_{aff}(\gamma) = \int_0^{r_c} w(\boldsymbol{r},\gamma)4\pi r^2 dr$$
$$= 4\pi \int_0^{r_c} w_0(\boldsymbol{r}) \exp(-\gamma^2 r^2/2\langle r^2\rangle_{aff}) r^2 dr \tag{6}$$

where $4\pi r^2\ dr$ is the volume element dV in Cartesian coordinate system. For small deformations, the value of this integral is approximately

$$n_{aff}(\gamma) \approx n_{aff}(0) \exp(-r_c^2\gamma^2/2\langle r^2\rangle_{aff}), \tag{7}$$

or, in terms of the critical force f_c from Eq. (5),

$$n_{aff}(\gamma) \approx n_{aff}(0) \exp[-(f_c/3kT)^2\langle r^2\rangle_{aff}\gamma^2/2] \tag{8}$$

where $n_{aff}(0)$ is given as

$$n_{aff}(0) = 4\pi \int_0^{r_c} w_0(\boldsymbol{r}) r^2 dr \tag{9}$$

and represents the fraction of unbroken linkages in unstrained state. It is worth noting that $n_{aff}(0)$ does not equal unity, which can be attributed to thermal breakdown of linkages in the moment of formation.

Equations (7) and (8) show what low strain functional dependence of G' (proportional to linkage density) would be like, if all network chains were equally long, with $\langle r^2\rangle = \langle r^2\rangle_{aff}$, since the length of a chain is proportional to its $\langle r^2\rangle$.

But according to assumption 2 all network chains are not of equal length and chain vector transformations of those with $\langle r^2\rangle \neq \langle r^2\rangle_{aff}$ are nonaffine in strain. However, deformation ratio, say λ', of such chain vectors is related to deformation ratio of affinely transformed vectors λ through the relationship between their corresponding relative deformations $\varepsilon'(\varepsilon' = \lambda' - 1)$ and $\varepsilon(\varepsilon = \lambda - 1)$, respectively, as

$$\varepsilon' = \varepsilon\langle r^2\rangle_{aff}^{1/2}/\langle r^2\rangle^{1/2}. \tag{10}$$

Considering this equation and the fact that for small $\varepsilon\ \gamma = \lambda - \lambda^{-1} = 1 + \varepsilon - (1+\varepsilon)^{-1} \approx 2\varepsilon$, replacement of γ in Eq. (8) by the expression

$\gamma\langle r^2\rangle_{aff}^{1/2}/\langle r^2\rangle^{1/2}$ would make Eq. (10) valid also for network chains of an arbitrary $\langle r^2\rangle$. The fraction of unbroken linkages in this generalized case, $n_g(\gamma)$, is then

$$n_g(\gamma) \approx n_g(0)\exp[-(f_c\langle r^2\rangle_{aff}/3kT)^2\gamma^2/2\langle r^2\rangle]. \tag{11}$$

This equation is sensible because it demonstrates that for shorter chains the necessary critical force to break secondary linkages is attained at lower strains than that for longer chains. In other words, the density of secondary linkages with shorter pendent chains decreases faster with increasing strain than that with the longer ones, which is plausible regarding the assumptions of this model.

In order to obtain the total fraction of still existing secondary linkages at a given strain, it is necessary to account for differences in chain lengths within the secondary network. Distribution of corresponding average chain vector values, $\langle r^2\rangle^{1/2}$, is assumed to be Gaussian (assumption 2), possessing the following form:

$$w(\langle r^2\rangle^{1/2}) = (3/2\pi\langle\bar{r}^2\rangle)^{3/2}\exp(-3\langle r^2\rangle/2\langle\bar{r}^2\rangle), \tag{12}$$

where $\langle\bar{r}^2\rangle$ is the overall average of the chain vector mean squares in the network. The total fraction of unbroken linkages at the strain γ is given by combination of Eq. (11) and distribution (12) as

$$n(\gamma) = 4\pi\int_0^\infty w(\langle r^2\rangle)^{1/2})n_g(\gamma)\langle r^2\rangle d\langle r^2\rangle^{1/2} \tag{13}$$

where integration is carried out over the entire space, since $\langle r^2\rangle^{1/2}$ can theoretically assume any value. When substituted for $w(\langle r^2\rangle^{1/2})$ and $n_g(\gamma)$, this integral assumes the form

$$n(\gamma) = A\int_0^\infty \langle r^2\rangle^{1/2}\exp(-a\langle r^2\rangle - b\gamma^2/\langle r^2\rangle)d\langle r^2\rangle \tag{14}$$

where $a \equiv 3/2\langle\bar{r^2}\rangle$, $b \equiv (f_c\langle r^2\rangle_{aff}/3kT)^2/2$ and $A \equiv 2\pi n(0)\,(3/2\pi\langle\bar{r^2}\rangle)^{3/2}$. Its evaluation yields the following final results:

$$n(\gamma) = n(0)(1 + c\gamma)\exp(-c\gamma) \tag{15}$$

and

$$-dn(\gamma)/d\gamma = n(0)c^2\gamma\exp(-c\gamma) \tag{16}$$

where $c \equiv f_c \langle r^2 \rangle_{aff} / 3^{1/2} \langle \bar{r^2} \rangle^{1/2} kT$, representing a dimensionless and for low strains a strain independent quantity. Multiplying the numerator and the denominator of this expression by the Avagadro number, N_A, it is immediately conceivable that the constant c can be rewritten as $c \equiv W_b / 3^{1/2}\, RT$ where R is the gas constant and

$$W_b \equiv N_A f_c \langle r^2 \rangle_{aff} / \langle \bar{r^2} \rangle^{1/2}, \tag{17}$$

a quantity with the unit of energy per mol, characteristic of material, which may be named *characteristic energy for secondary linkage breakdown* and subsequently *secondary network breakdown*. It can be easily determined from the measured dynamic mechanical functions and, as shown later, its values are typically within the range of energies characteristic for secondary interactions.

Being proportional to the linkage density in the network and thus to the total fraction of unbroken linkages at a given strain, $G'(\gamma)$ is then given as dictated by Eq. (15):

$$G'(\gamma) = G'(0)(1 + W_b \gamma / 3^{1/2} RT) \exp(-W_b \gamma / 3^{1/2} RT) \tag{18}$$

where G' (0) is the initial storage shear modulus, *i.e.*, at $\gamma = 0$.

At a given strain, $G''(\gamma)$ is proportional to deformational change of the total fraction of unbroken linkages and thus dictated by Eq. (16). As the function given by Eq. (16) experiences maximum at $\gamma_{\max} = c^{-1}$, *i.e.*, at the strain amplitude of the strongest decrease of secondary linkage density, $G''(\gamma)$ can be written in terms of its maximum value, $G''_{\max}$(at $\gamma_{\max}$), as

$$G''(\gamma) = G''_{\max}(W_b \gamma / 3^{1/2} RT) \exp(1 - W_b \gamma / 3^{1/2} RT). \tag{19}$$

The functions $G'(\gamma)$ and $G''(\gamma)$ as given by Eqs. (18) and (19), *i.e.*, with strain independent W_b, possess the very forms demonstrated in Figure 1. But their validity is limited to low strains because only for low strain values approximations made in deriving them are possible. The reason they well describe the strain induced breakdown of carbon black secondary agglomeration network in rubbers is that the entire process shown by Figure 1 in that case occurs in the low strain region (up to $\gamma \approx 0.2$) [4].

For polar rubbers and other polar rubber-based systems, such as NBR/TPU blends, the strain range for secondary network breakdown is much larger, although of similar form. This, in fact, is the incentive to extend the validity of existing equations to higher strains [7].

Indeed, Eqs. (18) and (19) may be used for higher strains as well, but in this case the characteristic breakdown energy W_b becomes strain dependent $W_b(\gamma)$. Although mathematically formal, the reason for this has also a physical explanation.

As the secondary linkages break and vanish with increasing strain, the average distance between still existing topologically adjacent linkages increases, making the denominator of the right-hand side of identity (17) ever larger. Plausibly assuming the critical force f_c to be independent of strain, this makes $W_b(\gamma)$ to decrease from its initial value $W_b(0)$ toward a low terminal value $W_b(\infty)$, when the network is destroyed. Its functional form may be obtained by the following next few steps.

Experimental evidence reveals that except at very low strains, the right-hand side of Eq. (15) is governed by the exponential term. Accounting for this, combination of Eqs. (15) and (16) gives approximately

$$dn(\gamma)/n(\gamma) \approx -W_b(\gamma)d\gamma/3^{1/2}RT. \tag{20}$$

Next, from the evident relation

$$n(\gamma)\langle \bar{\boldsymbol{r}^2}\rangle_\gamma^{3/2} = \text{const.}, \tag{21}$$

where $\langle \bar{\boldsymbol{r}^2}\rangle_\gamma^{3/2}$ represents the basic volume element associated with a linkage at shear strain γ, it follows that

$$dn(\gamma)/n(\gamma) = -d\langle \bar{\boldsymbol{r}^2}\rangle_\gamma^{3/2}/\langle \bar{\boldsymbol{r}^2}\rangle_\gamma^{3/2}. \tag{22}$$

Finally, identity (17) provides the relation

$$dW_b(\gamma)/W_b(\gamma) = -d\langle \bar{\boldsymbol{r}^2}\rangle_\gamma^{1/2}/\langle \bar{\boldsymbol{r}^2}\rangle_\gamma^{1/2}. \tag{23}$$

Combination of Eqs. (20), (22) and (23) yields the equation

$$dW_b(\gamma)/W_b^{\,2}(\gamma) = -d\gamma/3^{3/2}RT \tag{24}$$

from which, when integrated from $W_b(0) - W_b(\infty)$ at $\gamma = 0$ to $W_b(\gamma) - W_b(\infty)$ at γ and after rearrangement, the following functional form for $W_b(\gamma)$ is obtained:

$$W_b(\gamma) = W_b(\infty) + \{1/[W_b(0) - W_b(\infty)] + \gamma/3^{3/2}RT\}^{-1}. \tag{25}$$

The constants $W_b(0)$ and $W_b(\infty)$ can simply be determined from the measured $G'(\gamma)$ and Eq. (18). For low strains the exponential term of the right-hand side of Eq. (18) can be expanded into series, and, keeping the first two terms, the equation turns into

$$G'(\gamma) \approx G'(0)[1 - W_b(0)^2\gamma^2/3(RT)^2] \tag{26}$$

from which $W_b(0)$ can easily be calculated.

At high strains $W_b(\gamma)$ becomes $W_b(\infty)$ and Eq. (18) can be approximated by

$$G'(\gamma) \approx G'(0)[W_b(\infty)\gamma/3^{1/2}RT] \exp[-W_b(\infty)\gamma/3^{1/2}RT]. \tag{27}$$

Using this equation, $W_b(\infty)$ can simply be determined from the slope of the linear plot $ln[G'(\gamma)/\gamma]$ *vs.* γ.

With so-determined $W_b(0)$ and $W_b(\infty)$ substituted in Eq. (25) and this in turn in Eqs. (18) and (19) excellent agreement of the model is obtained with the measured $G'(\gamma)$ over the whole strain range. As predicted, in the case of $G''(\gamma)$ the agreement with experiment is poorer, particularly at low strains, because the model does not account for internal friction. Nevertheless, the model correctly predicts the strain amplitude shift of $G''_{\max}$ for different temperatures and TPU contents in NBR/TPU blends. Specifically, $G''_{\max}$ is expected to shift toward lower strain amplitudes with increasing both temperature and volume fraction of TPU. In the first case, the reason is that due to intensified thermal molecular motion at elevated temperatures, the critical force for linkage breakdown, f_c, given by Eq. (5), is attained at lower strains. In the second case, the same is true because increasing content of TPU produces higher secondary linkage density in blends, making the topologically adjacent linkages to be closer to one another and thus the attainment of the force necessary to break them at ever lower strains.

The functions $G'(\gamma)$ and $G''(\gamma)$ as given by Eqs. (18) and (19) tend toward zero when $\gamma \to \infty$, although in reality they decrease toward low but finite values $G'(\infty)$ and $G''(\infty)$, respectively. At high strains, the secondary network is practically destroyed, but some secondary linkages may still form and almost instantly disappear, whereas to finite values of dynamic functions may also contribute some remaining molecular entanglements. So, strictly, Eqs. (18) and (19) should be written in terms of functional differences rather than functions alone, *i.e.*, $G'(\gamma) - G'(\infty)$ and $G'(0) - G'(\infty)$ in Eq. (18), as well as $G''(\gamma) - G''(\infty)$ and $G''_{\max} - G''(\infty)$ in Eq. (19). But since for all sensible

strains $G'(\gamma) \gg G'(\infty)$ and $G''(\gamma) \gg G'(\infty)$, the forms of Eqs. (18) and (19), as written, are satisfactory.

Finally, it is worth mentioning that good agreement of this model (which accounts for the secondary network breakdown only) with experiment in the case of G' rules out any effects of nonlinear viscoelasticity from being responsible for strain dependence of G'. This concurrently confirms the fact predicted by the finite strain rheology that, unlike in the case of extension, the stress-strain relation in simple shear remains linear at finite strains, with strain independent shear modulus [10].

2.2. Effect of Temperature

The theory of rubber elasticity predicts the storage shear modulus to be proportional to the density of network chains, N, and temperature in the following manner [5]: $G' = NkT$. For perfect networks, N, in turn, is related to the linkage density n as $N = \varphi n/2$ where φ is the average functionality of the linkages [11]. This makes the storage modulus proportional to the linkage density: $G' \propto nkT$. But in the case of secondary network, the linkage density itself depends on temperature, owing to the thermal molecular motion. At given temperature secondary linkages form and decay in a dynamic equilibrium, their average density being constant. Upon temperature change, a new equilibrium is established at another linkage density.

It is not difficult to envision an energy barrier that must be surpassed for a linkage to break (assumption 3). Indeed, experimental evidence suggests the decrease in linkage density with increasing temperature to be a thermally activated process, *i.e.*, $n \propto \exp(E_a/RT)$ where E_a is the value of the energy barrier height and may be named the *activation energy for secondary linkage breakdown* and subsequently for *secondary network thermal breakdown*. Taking account of this, $G'(T)$ has then the following form:

$$G'(T) = CT \exp(E_a/RT) \tag{28}$$

where C is a constant. For polar blends, such as NBR/TPU, this relation holds with high precision. E_a can simply be obtained from the slope of the plot $ln[G'(T)/T]$ *vs.* $1/T$.

$G''(T)$, too, decreases with increasing temperature, but since to this decrease also contributes reduction of internal friction, it is difficult, primarily at low strains, to assess individual contributions. However, according to Eqs. (15) and (16) $G'_{\gamma=0}$ (at zero strain amplitude) and $G''_{\max}$

should be proportional to each other and so the functional form of the latter should be the same as that of $G'_{\gamma=0}(T)$.

With increasing temperature the strain amplitude γ_{max} of the maximum in G'' is expected to be shifted toward lower values. The functional form $\gamma_{max}(T)$ can be obtained by examining the quantity $c \equiv W_b/3^{1/2}RT$ from Eqs. (15) and (16), since for low strains $\gamma_{max} = c^{-1}$. Due to different temperature dependences of the numerator and denominator at the right-hand side of identity (17), the characteristic energy W_b increases with increasing temperature linearly as $W_b(T) = k_1T - k_2$ where k_1 and k_2 are constants. For $\gamma_{max}(T)$ it then follows approximately:

$$\gamma_{max}(T) \approx 3^{1/2}R(k_1 - k_2/T)^{-1} \tag{29}$$

and for low values of the expression k_2/k_1T,

$$\gamma_{max}(T) \approx 3^{1/2}Rk_1{}^{-1}\exp(k_2/k_1T). \tag{30}$$

2.3. Effect of Composition

TPU in NBR/TPU blends is expected to act reinforcingly by introduction of additional secondary linkages, resulting in higher network chain density N. Analysing the effect of TPU volume fraction in the blends, ϕ, it can be plausibly assumed that $d\langle\bar{r^2}\rangle^{3/2} \propto -d\phi$ and in turn, considering Eq. (21), $dn/n^2 \propto d\phi$. For small ϕ's, integration of this yields the following dependence of secondary linkage density on volume fraction of TPU: $n(\phi) \approx n(\phi = 0)(1 + K\phi) \approx n(\phi = 0)\ \exp(K\phi)$ where K is a constant characteristic of material. Assuming the average functionality of the linkages, φ, to remain unchanged by the addition of TPU and since G' is proportional to n, the functional form of $G'(\phi)$ for low values of ϕ is:

$$G'(\phi) \approx G'(\phi = 0)\exp(K\phi). \tag{31}$$

Again, due to mutual proportionality, G''_{max} should possess the same functional form as $G'_{\gamma=0}(\phi)$. With increasing volume fraction of TPU the strain amplitude γ_{max} of the maximum in G'' is expected to decrease. Analysing again the expression c from Eqs. (15) and (16), it turns out with the help of Eq. (5) that W_b is approximately proportional to $\langle\bar{r^2}\rangle^{-3/2}$ and γ_{max} subsequently to $\langle\bar{r^2}\rangle^{3/2}$. Its functional dependence on the volume fraction of TPU is then:

$$\gamma_{\max}(\phi) \approx \gamma_{\max}(\phi = 0)(1 - K'\phi) \tag{32}$$

where K' is another constant. For low values of ϕ this equation turns into

$$\gamma_{\max}(\phi) \approx \gamma_{\max}(\phi = 0)\exp(-K'\phi). \tag{33}$$

3. EXPERIMENTAL

The Experimental part of this work comprises preparation of NBR blends with 10, 30 and 50 phr (parts in weight per hundred parts of rubber) of TPU in accordance with the standard ASTM D 3185-82, but without fillers. As a rubber base in the blends, NBR (Krynac, Polysar, 27 wt.% acrylonitrile) of weight average molecular weight 373000 g mol^{-1} was used, whereas TPU (Elastolan C 90 A, Bayer) used in the blends possessed weight average molecular weight of 170000 g mol^{-1}. Dynamic mechanical functions G' and G'' of the blends were then measured as a function of shear strain amplitude and temperature by the instrument Rubber Process Analyser–RPA 2000, Alpha Technologies. Measurements were carried out at the frequency of 0.3 Hz which is low enough to permit undisturbed changes of molecular conformations in the entire chosen range of strain (from 0.01 to 9) and that of temperature (from 30°C to 100°C). Using Eqs. (26) and (27), characteristic energies $W_b(0)$ and $W_b(\infty)$ for the secondary network mechanical breakdown were determined from the G'-values at low and high strain amplitudes, respectively. With these energies $G'(\gamma)$ and $G''(\gamma)$ were calculated by Eqs. (18) and (19) and compared with the measured ones. The agreement would confirm the existence of secondary networks in NBR/TPU blends, as well as credibility of the model itself.

Pertaining to the secondary network thermal breakdown, validity of Eq. (28) was examined by checking for linearity of the plots $ln\lfloor G'_{\gamma=0}(T)/T\rfloor$ *vs.* $1/T$ for blends of different TPU contents, from which the corresponding activation energies E_a could then be obtained. Proportionality of $G'_{\gamma=0}$ and $G''_{\max}$ was tested by comparing plots of $ln\lfloor G'^{\gamma=0}(T)/T\rfloor$*vs.* $1/T$ and $ln[G''_{\max}(T)/T]$ *vs.* $1/T$. Additionally, Eq. (30), describing temperature dependence of $\gamma_{\max}$, was verified by plotting $ln\,\gamma_{\max}\,(T)$ *vs.* $1/T$ for blends of different TPU contents.

Finally, the predicted effect of the blends' composition was verified by examining validity of Eq. (31), *i.e.*, by plotting $ln\,G'_{\gamma=0}(\phi)$ *vs.* ϕ at different temperatures and looking for linearity which would enable determination of the constant K. Here, too, proportionality of $G'_{\gamma=0}$ and

G''_{max} was tested by comparing plots of $ln\, G'_{\gamma=0}(\phi)$ *vs.* ϕ and $ln\, G''_{max}(\phi)$ *vs.* ϕ. As in the case of temperature dependence, γ_{max} as a function of TPU content, as described by Eq. (33), was verified by plots of $ln\, \gamma_{max}\,(\phi)$ *vs.* ϕ for blends at different temperatures.

4. RESULTS AND DISCUSSION

4.1. Effect of Strain

Figure 2 demonstrates strain amplitude dependence of G' for the NBR blend with 50 phr TPU at different temperatures. Points and curves represent measured and by the model calculated $G'(\gamma)$, respectively. Good agreement is obtained in all the cases over the whole strain amplitude range and at all temperatures. Furthermore, the effect of temperature gradually diminishes with increasing strain, to disappear entirely at high strains when the secondary network is destroyed, exactly as predicted by the model.

The corresponding values of characteristic energies W_b (0) and W_b (∞) given in the figure are within range typical for secondary interaction energies. As can be seen, $W_b(0)$ increases with temperature. This is because in identity (17) the critical force for the secondary linkage breakdown f_c (given by Eq. (5)) increases with increasing

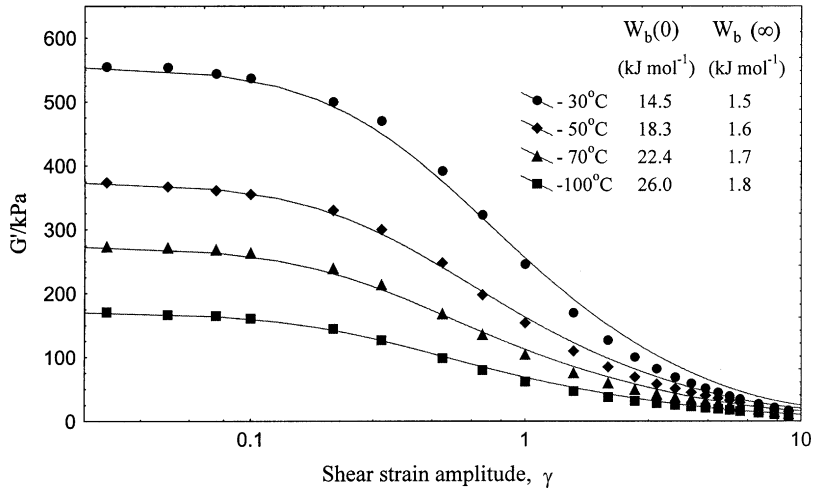

FIGURE 2 Shear strain amplitude dependence of storage shear modulus for NBR/TPU blend of 50 phr TPU content at the frequency of 0.3 Hz and different temperatures (measured: points, calculated: curves).

temperature faster than the denominator term $\langle \bar{r}^2 \rangle^{1/2}$ does. On the other hand, since at very high strains the secondary network is destroyed, the expression $W_b(\infty) / 3^{1/2} RT$ is constant and, therefore, $W_b(\infty)$ increases only slightly with increasing temperature.

Strain amplitude dependence of G'' at different temperatures is demonstrated in Figure 3 for NBR blends with 50 phr TPU. As emphasized earlier, agreement of experiment with the model in the case of G'', *i.e.*, Eq. (19), is expected to be worse, particularly at low strains, because the model does not consider another important energy dissipation mechanism, the internal friction. Besides, at low strains the secondary linkage breakdown is not yet expressed enough and hence screened. At higher strains, though, particularly at those beyond the strain of G''_{max}, the secondary linkage decay becomes intense, while internal friction is lessened, owing to increasing degree of molecular alignment. This makes the former the dominant energy dissipation mechanism, resulting in improved agreement of the model with experiment.

Figures 4 and 5 demonstrate $G'(\gamma)$ and $G''(\gamma)$, respectively, of NBR/TPU blends with different TPU contents at the temperature of 30°C. Here, too, good agreement of the model with experiment is obtained over the whole strain range in the case of $G'(\gamma)$, while for the foregoing reason the agreement of the calculated $G''(\gamma)$ with

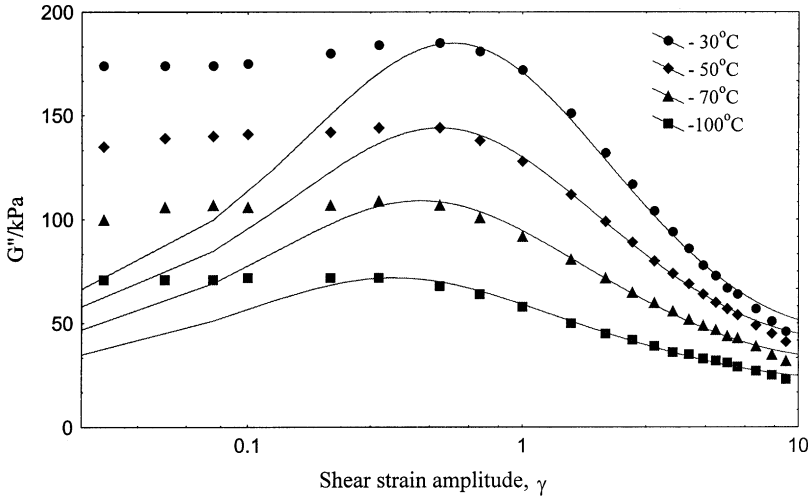

FIGURE 3 Shear strain amplitude dependence of loss shear modulus for NBR/TPU blend of 50 phr TPU content at the frequency of 0.3 Hz and different temperatures (measured: points, calculated: curves).

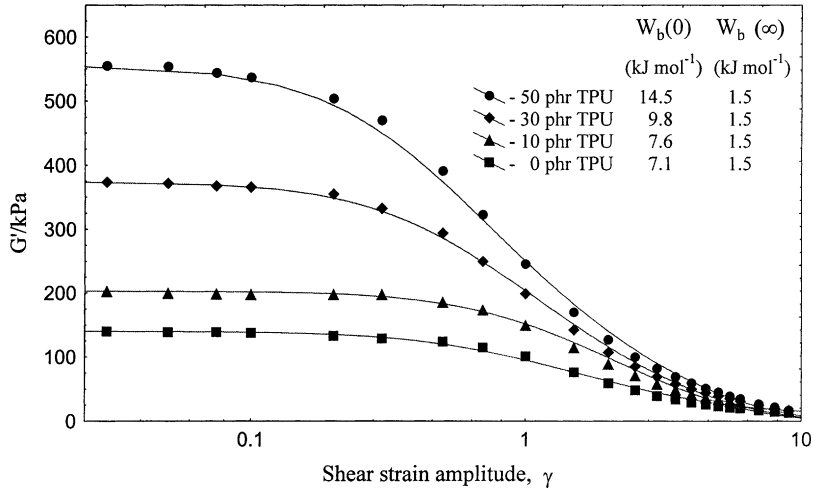

FIGURE 4 Shear strain amplitude dependence of storage shear modulus for NBR/TPU blends of different TPU contents at the frequency of 0.3 Hz and temperature of 30°C (measured: points, calculated: curves).

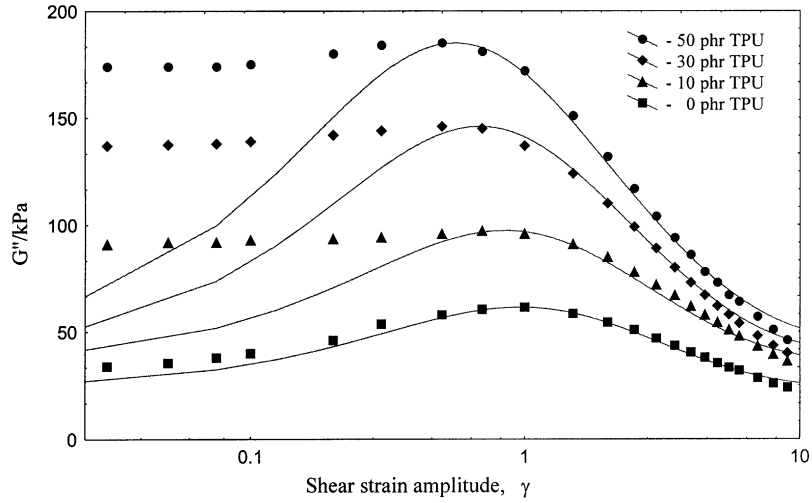

FIGURE 5 Shear strain amplitude dependence of loss shear modulus for NBR/TPU blends of different TPU contents at the frequency of 0.3 Hz and temperature of 30°C (measured: points, calculated: curves).

measurements is attained at higher strains only. As can be seen, TPU acts in NBR reinforcingly at low strains, but this effect diminishes with increasing strain and ultimately vanishes completely, when the secondary network is destroyed.

The characteristic energy W_b (0) moderately increases with increasing TPU content, presumably due to closer electric dipole packing, whereas $W_b(\infty)$, on the other hand, logically remains unchanged.

4.2. Effect of Temperature

Eq. (28) predicts linear relationship between the expressions $ln[G'(T) / T]$ and $1/RT$, the slope of the plot representing the activation energy for secondary network thermal breakdown, E_a. This is shown in Figure 6 for NRR/TPU blends of different TPU contents. Since with increasing strain the differences between the blends' $G'(\gamma)$ at different temperatures diminish, as demonstrated in Figure 2, E_a also decreases, to become zero at very high strains, when $G'(\gamma)$ assumes the temperature independent low value $G'_{\gamma=\infty}$. As a quantity characterizing the secondary network thermal breakdown is therefore chosen E_a obtained from the initial storage moduli $G'_{\gamma=0}$ at different temperatures.

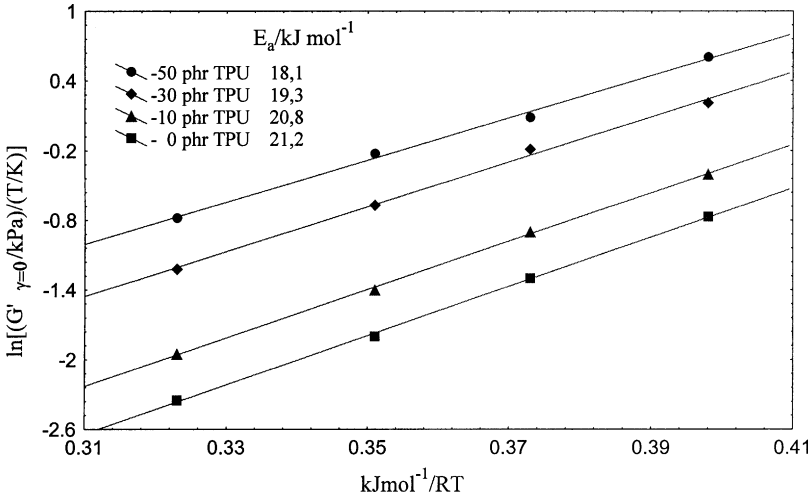

FIGURE 6 Plots of $ln(G'_{\gamma=0}/T)$ against 1/RT for storage shear moduli of NBR/TPU blends with different compositions.

It is clear from the figure that linear relationship of high correlation is obtained in all the cases. The activation energies are all within the energy range characteristic for secondary interactions. They slightly decrease with increasing TPU content, which can be attributed to gradual thermal stabilization of the secondary network by TPU.

Figure 7 demonstrates comparison of $G'_{\gamma=0}(T)$ and $G''_{\max}(T)$ which should, according to the model, be proportional to each other. The taken moduli values are for the blend of 50 phr TPU content. If $G'_{\gamma=0}$ and $G''_{\max}$ were strictly proportional to each other, the logarithmic plots $ln\lfloor G'_{\gamma=0}(T)/T\rfloor$ *vs.* $1/T$ and $ln[G''_{\max}(T)/T]$ *vs.* $1/T$ given in the figure would be parallel. Despite high correlation linearity of the plots obtained in both cases, the slopes slightly differ. This can be ascribed to intesification of internal friction with decreasing temperature, which results in somewhat lower slope in the case of $G''_{\max}(T)$.

The shift of $G''_{\max}$ toward lower strain amplitudes with increasing temperature is clearly seen on Figure 3 and predicted by Eq. (30). Figure 8 demonstrates plots of $ln\gamma_{\max}(T)$ *vs.* $1/T$ for blends of different TPU contents. Good agreement is obtained in all the cases, confirming validity of Eq. (30).

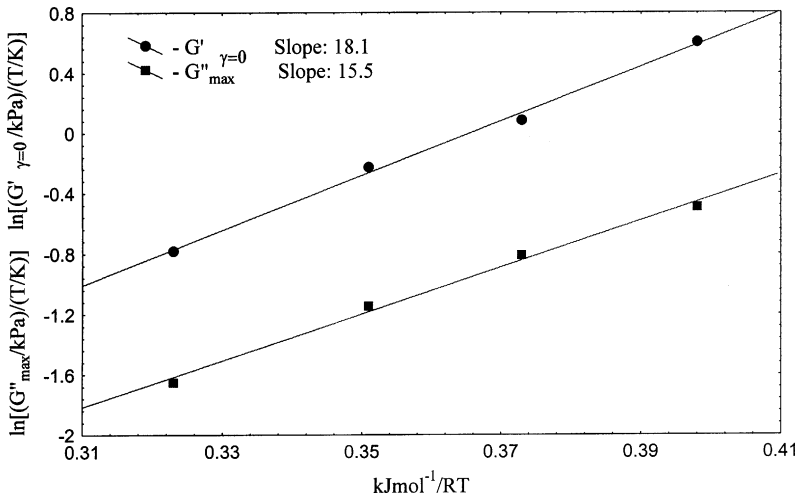

FIGURE 7 Examination of proportionality of $G'_{\gamma=0}$ and $G''_{\max}$ for NBR/TPU blend of 50 phr TPU content through plots of $ln(G'_{\gamma=0}/T)$ and $ln(G''_{\max}/T)$ *vs.* $1/RT$, respectively.

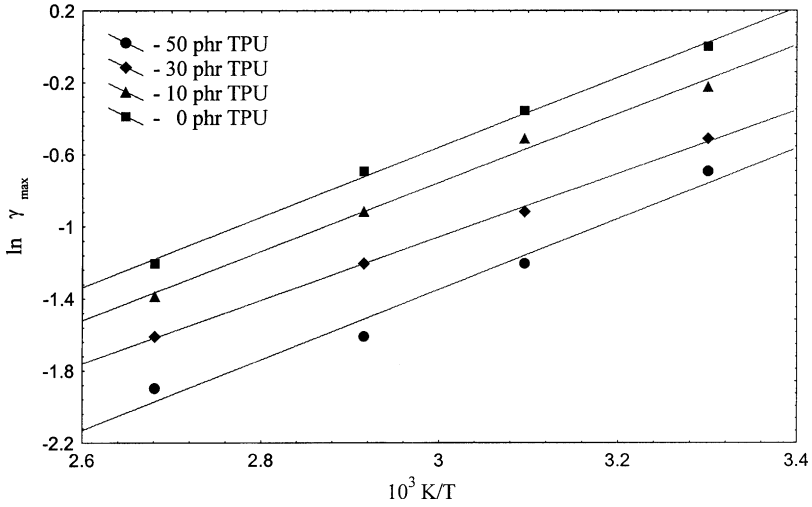

FIGURE 8 Temperature dependence of shear strain amplitude γ_{max} (at which G''_{max} is attained) for NBR/TPU blends of different compositions.

4.3. Effect of Composition

Reinforcing effect of TPU in NBR/TPU blends and their vulcanizates is already evident from Figures 3 and 4. To verify its quantitative prediction, *i.e.*, Eq. (31), plots of lnG' (ϕ) (G' taken at zero strain amplitude) *vs.* volume fraction of TPU ϕ are made for different temperatures, as shown in Figure 9. Linear relationship of high correlation confirms the accepted assumptions on the effect of blends' composition. As can be seen, the constant K slightly increases with increasing temperature. This is presumably due to stronger thermal molecular motion at higher temperatures, causing lower secondary linkage density and thus making more space available for new linkages to form. The result is a stronger *relative* increase of linkage density with increasing amount of TPU at higher temperatures than the one at lower temperatures.

Similarly to Figure 7, examining proportionality of $G'_{\gamma=0}$ and G''_{max} at different temperatures, Figure 10 shows comparison of these moduli of blends with different TPU contents at 30°C. Again, the plots, this time of $ln\, G'_{\gamma=0}(\phi)$ *vs.* ϕ and $ln\, G''_{max}(\phi)$ *vs.* ϕ, are linear, as predicted, but somewhat unparallel. The slope in the case of $G''_{max}(\phi)$ is lower due to intesifying internal friction, this time with increasing TPU content.

The shift of G''_{max} toward lower strains with increasing TPU content, as predicted by Eq. (33), is immediately perceivable on Figure 4.

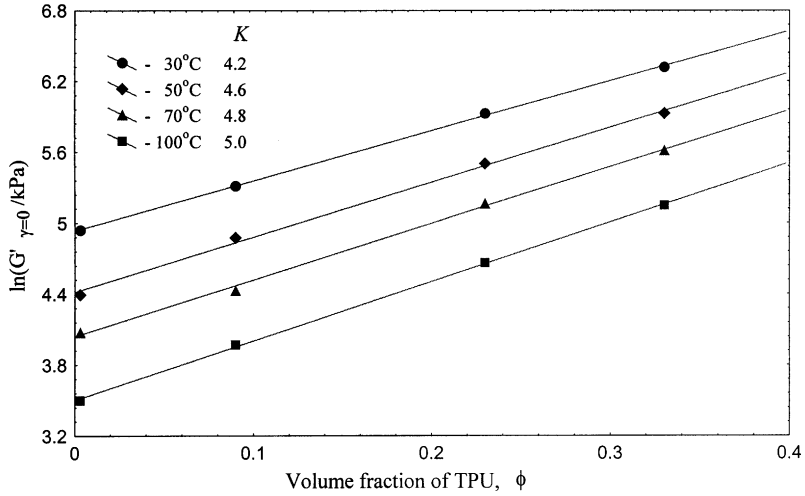

FIGURE 9 Dependence of zero strain amplitude storage moduli $G'_{\gamma=0}$ of NBR/TPU blends on volume fraction of TPU at different temperatures.

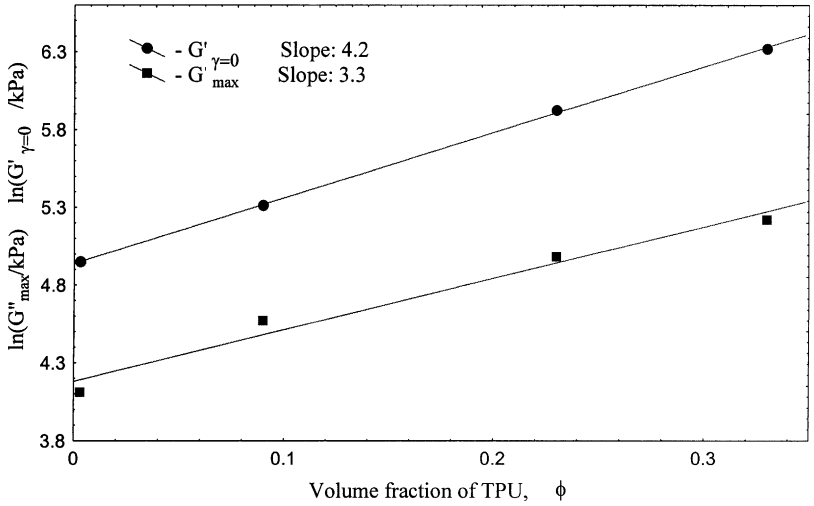

FIGURE 10 Examination of proportionality of $G'_{\gamma=0}$ and $G''_{\max}$ at the temperature of 30°C through plots of $ln\, G'_{\gamma=0}$ and $ln\, G''_{\max}$ *vs.* volume fraction of TPU in NBR/TPU blends, respectively.

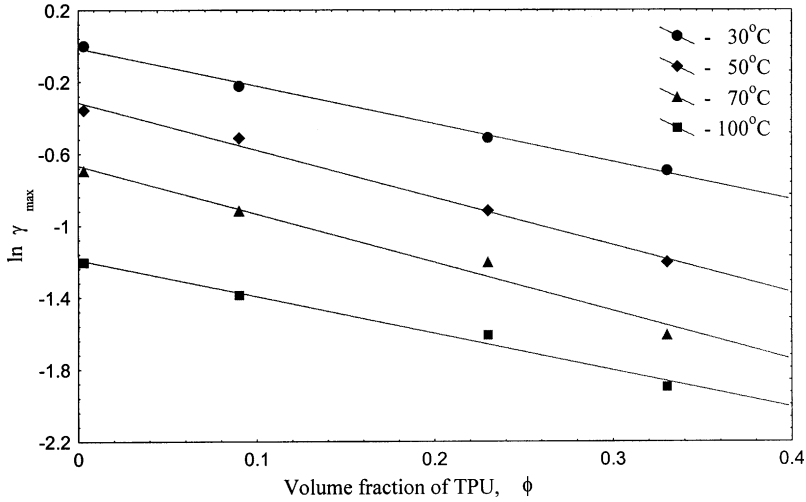

FIGURE 11 Dependence of shear strain amplitude γ_{max} (at which G''_{max} is attained) on volume fraction of TPU in NBR/TPU blends at different temperatures.

Figure 11 shows plots $ln\,\gamma_{max}\,(\phi)$ *vs.* ϕ at different temperatures. Once more, high correlation linear relationship is obtained in all the cases, v indicating Eq. (33).

5. CONCLUSION

Several important results have been obtained by relating rheological properties of polar polymer blends with their secondary morphological structures. Good qualitative and quantitative agreement with experiment of the proposed theoretical model for strain, temperature and compositional dependence of the blends' dynamic mechanical functions substantiates both the very existence of secondary networks formed by secondary interactions in these materials and the assumptions on which the model is based. Furthermore, by the agreement of the model with experiment, means are provided to determine two energies characterizing the secondary networks: the characteristic energy for network's strain induced breakdown and activation energy for its thermal breakdown. The values of these energies are of the magnitudes typical for energies of secondary interactions. The model also enables determination of a characteristic material constant pertaining to compositional dependence of the blends' dynamic functions. And finally, although in this work the

model is used to describe rheological properties of NBR/TPU blends in terms of their secondary morphology, the model itself is rather general, since it is not associated with any specific polar polymer blends—after all, it was originally devised to study carbon black secondary agglomeration networks in rubbers. So, likely, dynamic mechanical functions or other equivalent and easily measured rheological quantities could be used in conjunction with the model to study morphology and its association with reological properties of any related materials, including covalently crosslinked ones.

REFERENCES

[1] Painter, P. C. and Coleman, M. M. , *Fundamentals of Polymer Science* (Technomic Publ. Co., Lancaster, 1997), Chap. 7, pp. 212–217.
[2] Frenkel, D., In; *Soft and Fragile Matter* (Cates, M. E. and Evans, M. R. Eds.), (SUSSP Publications and Institute of Physics Publishing, Edinburg, London, 2000), pp. 115–119.
[3] Graessley, W. W. (1974). *Adv. Polym. Sci*. **16**, 1.
[4] Susteric, Z. (1989). *Makromol. Chem., Makromol. Symp*. **23**, 329.
[5] Ward, I. M. and Hadley, D. W., *An Introduction to the Mechanical Properties of Solid. Polymers* (Wiley, New York, 1993), Chap. 3, pp. 32–40.
[6] Ferry, J. D.,*Viscoelastic Properties of Polymers* (Wiley, New York, 1980), Chap. 12, pp. 328–343.
[7] Susteric Z. *et al.* (1999). *Acta Chim. Slov.* **46**, 69.
[8] Flory P. J. (1976). *Proc. R. Soc. Lond*. **A.351**, 351.
[9] Treloar L. R. G. , (1974). *Rubber Chem. Technol*. **47**, 625.
[10] Vinogradov, G. V. and Malkin, A. Ya., *Rheology of Polymers* (Mir, Moscow, 1980), Chap. l, pp.
[11] Mark, J. E. and Erman, B., *Rubberlike Elasticity a Molecular Primer* (Wiley, New York, 1988), Chap. 3, pp. 26–27.